

Flexural strength of fused filament fabricated (FFF) PLA parts on an open-source 3D printer

Shilpesh R. Rajpurohit¹ · Harshit K. Dave¹

Received: 3 July 2018 / Accepted: 22 October 2018 / Published online: 13 November 2018
© Shanghai University and Springer-Verlag GmbH Germany, part of Springer Nature 2018

Abstract Fused filament fabrication (FFF) has been widely used to develop prototypes as well as functional parts owing to its capability for creating parts with complex geometries in a short time without the specific requirement of tooling. The mechanical properties of parts produced by FFF exhibit 70%–80% of the mechanical properties of parts produced by injection molding. The mechanical properties of FFF-produced parts are primarily dependent on the selection of various process variables. The mechanical properties of the part can be enhanced through the proper selection of process variables. In the present experimental investigation, the effects of the process variables, viz. raster angle, layer height, and raster width on the flexural properties of FFF-printed polylactic acid (PLA) is studied. The result shows that flexural strength is primarily influenced by layer height followed by raster angle. The sample printed with 100- μm layer height and 0° raster angle exhibits a higher tensile strength. Further, the microscopic examination of the deformed specimen is performed to understand the mode of failure. Specimens printed at different raster angles show different modes of failure.

Keywords Fused filament fabrication (FFF) · Polylactic acid (PLA) · Raster angle · Layer height · Raster width · Flexural strength

1 Introduction

Additive manufacturing (AM) has evolved from the rapid prototyping to rapid manufacturing of end-use functional parts. AM is advantageous over other conventional manufacturing techniques in terms of fabricating part with complex geometries and integrated designs at low cost, without the need of specific tooling, and a shorter processing time. AM is used in various industries such as automobile, biomedical, aerospace, rapid tooling, and consumer product [1, 2].

Recently, various AM technologies including selective laser sintering, selective laser melting, electron beam melting, stereolithography, laminated object manufacturing, fused deposition modeling (FDM), and fused filament fabrication (FFF) have evolved to fabricate components layer by layer [3]. Among these additive manufacturing technologies, FFF is the most widely accepted method owing to its reliability, low cost, and simplicity. Material extrusion includes FFF processes that use different thermoplastic polymer materials to fabricate the component layer by layer. During the printing process, the filament material is fed into a heated nozzle that is extruded in a semi-liquid state, and deposited as a thin layer on to the previously deposited layer on the build platform, as defined by the sliced information. As the environment temperature is lower than the melting temperature of the material, the deposited material quickly solidifies and bonds to the adjacent layer. After one layer is deposited, the build platform moves downwards along the z-axis by the height of one layer thickness, and the process is repeated for the next layer [4–6]. However, owing to the inherent characteristic of the raster-by-raster and layer-by-layer forming process, FFF fabricated parts can exhibit lesser flexural properties owing to the insufficient bonding between

✉ Harshit K. Dave
harshitkumar@yahoo.com

¹ Department of Mechanical Engineering, S V National Institute of Technology, Surat, Gujarat 395 007, India

rasters and layers that may possibly cause the delamination effect, thus resulting in premature failure. This disadvantage restricts the application of FFF parts and leaves prototyping as the primary one [7]. The flexural properties of the FFF part can be improved by the proper selection of the process variables. The FFF process variables primarily influence the meso structural appearance, bonding between the layers, and rasters of the parts that ultimately affect the quality of the printed part.

Recently, researchers have studied the influence of the process variable on the flexural behavior of the FFF part to broaden the application field of FFF printed parts. Mishra et al. [8] observed that a number of external perimeters reduced the voids near the edge that increased the flexural strength. Luzanin et al. [9] investigated the effects of layer height, raster angle, percentage infill, extrusion speed, and extrusion temperature on the flexural strength of PLA parts, wherein experiments had been designed using the definitive screening design (DSD). They found that the highest flexural strength was observed at 0° raster angle. They reported a higher percentage infill that improved the flexural strength at a larger thickness and a higher extrusion speed. Mohamed et al. [10] studied the flexural creep stiffness behavior of FDM-processed PC-ABS parts. Flexural creep stiffness can be enhanced using a lower raster angle, a thinner layer, more perimeters, and a lower value of raster-to-raster air gap. Garg et al. [11] obtained a higher flexural strength at a lower value of raster angle because the deposited layer remained almost parallel to the bending plane that offered resistance to bending. Motaparti et al. [12] studied the effects of build direction, raster angle, and air gap on the flexural properties of the FDM part. They observed that a specimen built with 0°/90° raster angle with a negative air gap yielded higher flexural strength. Rahman et al. [13] studied the effect of raster angle (0°, 90°, and 0°/90°) on the tensile, flexural, and compressive strengths of FFF-produced PEEK materials. A higher flexural strength was obtained at 0° followed by 0°/90° and 90°. Christiyani et al. [14] also observed a higher flexural strength at 0° raster angle. However, the flexural strength was found to be decreased with an increment in the layer height. A unidirectional 0° raster angle achieved a higher flexural strength, as well as a negative air gap enhanced the flexural strength of printed specimens, as reported by Knoop et al. [15]. Sood et al. [16] studied the effects of various process variables (layer thickness, orientation, raster width, air gap, and raster angle) on the mechanical properties (tensile strength, flexural strength, and impact strength) of FDM-produced ABS parts. A higher flexural strength was obtained at a low value of raster angle, air gap, and layer thickness as well. Guan et al. [17] observed that flexural strength decreased with an increase in the air gap for both planar FDM and curved-

Table 1 Properties of PLA filament

Properties	Value
Density/(g·cm ⁻³)	1.20–1.25
Melt point/°C	190–220
Melt flow index, g/10 min	7.8
Tensile yield strength/MPa	62.63
Elongation at break/%	4.43
Flexural strength/MPa	65.02
Flexural modulus/MPa	2 504.4
Impact strength/(kJ·m ⁻²)	4.25
Accuracy/mm	1.75±0.05

Table 2 Variable process parameters

Parameters	Levels		
	1	2	3
Raster angle/(°)	0	45	90
Layer height/μm	100	200	300
Raster width/μm	500	600	700

Table 3 Fixed process parameters

Parameters	Value
Liquefier temperature/°C	210
Bed temperature/°C	70
Scan speed/(mm·s ⁻¹)	50
No. of perimeters	1
Infill/%	100
Infill pattern	Rectilinear

layer FDM. Dawoud et al. [18] studied the effect of raster angle and air gap on the flexural strength of the ABS part, and compared it to those of injection-molded parts. A negative air gap with a small raster angle yields a higher flexural strength that is 12% less than the flexural strength obtained with an injection-molded part. Durgun and Ertan [19] obtained a higher strength with a sample printed in the *x* and *y* orientations. They also reported that flexural strength decreased with an increment in the raster angle. Liu et al. [20] studied the effects of process variables (orientation, layer thickness, raster angle, raster width, and raster gap) on the mechanical properties (tensile strength, flexural strength, and impact strength) of FDM-produced PLA parts. Part printed in the *x*-direction with 0° raster angle exhibited a higher flexural strength. Huang et al. [21] observed that the build orientation and layer height

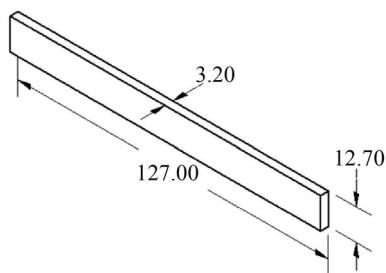
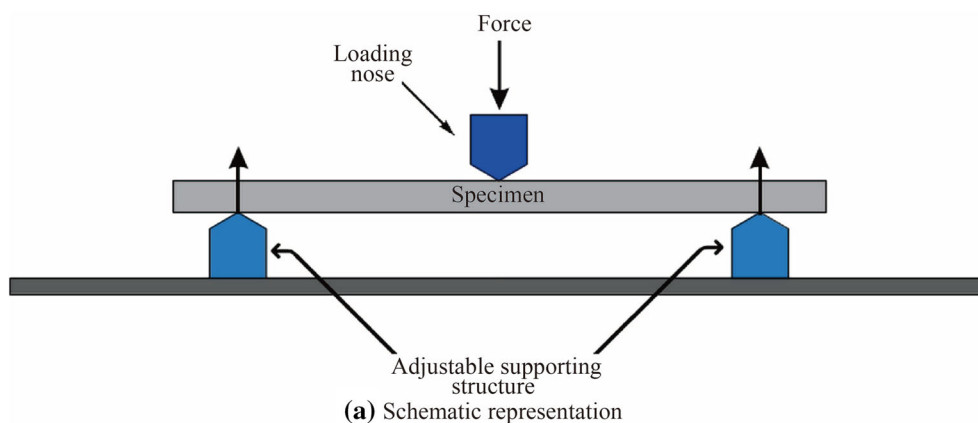


Fig. 1 Flexural test specimen (all dimensions are in mm)

significantly affected the flexural strength of the ABS-printed part. They also found that the raster angle did not pose a significant effect when printing using a bi-directional raster angle rather than a unidirectional raster angle. Es-Said et al. [22] observed the highest flexural strength with 0° layer orientation.

Previous works have suggested that the flexural properties of FFF parts may be affected by the different process parameters. An extensive review of the studies also suggest that few studies have been devoted to studying the

influence of process variables on the flexural strength of FFF-printed PLA parts. PLA is a widely used polymer in three-dimensional (3D) printing technologies. As PLAs exhibit excellent properties such as high strength, hardness, renewability, and low toxicity, it can reduce the consumption of petroleum-based polymers and improve the eco-friendliness of FFF-printed parts. The primary objective of the present research is to understand the flexural behavior of the PLA part printed by FFF, and to study the effects of the process variables including the raster angle, layer height, and raster width on the flexural properties of FFF-printed PLA parts. Further, the deformed specimen under flexural loading is microscopically examined to understand the failure mode of the specimen fabricated under different fabrication conditions.



(b) Test specimen before the test



(c) Test specimen after the test

Fig. 2 Experimental set up for flexural test

2 Materials and methods

2.1 Machine

An entry-level 3D printer, OMEGA Dual Extruder, was used to fabricate the flexural test specimens. The machine can build a part with a maximum volume of 500 mm × 500 mm × 500 mm. The machine has a positional accuracy of ±11 μm in the *x-y* axis and ±10 μm in the *z*-axis with a 0.4-mm nozzle diameter. The 3D printer can print materials with a maximum speed of 150 mm/s. Further, it can print various types of filament materials such as PLA, ABS, PVA, and Nylon of diameter 1.75 mm.

Initially, the CAD model of the test specimen is created using Pro E wildfire 5.0 and exported as an STL file. Subsequently, the STL file is transferred to the Repetier Host with Slice3r as the slicing engine. The Repetier Host

sliced the STL file to create tool pathways with the adjustment of all the process variables, and exported the instructions as a G Code file. The G Code file is subsequently transferred to the 3D Printer. The 3D printer fabricated the part by extruding the thermoplastic material by depositing layer by layer. Once the specimen has been prepared, it is replaced from the 3D printer, and the support structure (if any) is removed mechanically from part or chemically dissolving it to prepare the part.

2.2 Material

In the present investigation, PLA is selected as the filament material, which is a bio-based polymer that can be derived from renewable resources such as corn, potatoes, and sugar from beets, cassava roots, sugarcane, etc. The carbon dioxide formed during disposal, incineration or

Table 4 Experimental data obtained through experimental performance for flexural strength

Sr. no.	Raster angle/(°)	Layer height/μm	Raster width/μm	Flexural strength /MPa		Mean flexural strength/MPa	S/N ratio	Standard deviation
				Trial 1	Trial 2			
1	0	100	500	70.70	66.30	68.50	36.700 4	3.11
2	0	100	600	78.20	70.20	74.20	37.370 2	5.66
3	0	100	700	72.10	73.20	72.65	37.224 0	0.78
4	0	200	500	72.00	64.30	68.15	36.627 7	5.44
5	0	200	600	71.20	60.70	65.95	36.301 6	7.42
6	0	200	700	77.40	77.00	77.20	37.752 3	0.28
7	0	300	500	69.20	63.30	66.25	36.397 9	4.17
8	0	300	600	76.00	70.30	73.15	37.264 5	4.03
9	0	300	700	77.10	70.50	73.80	37.335 1	4.67
10	45	100	500	78.20	75.70	76.95	37.720 7	1.77
11	45	100	600	76.80	76.20	76.50	37.673 0	0.42
12	45	100	700	74.20	65.90	70.05	36.862 4	5.87
13	45	200	500	75.10	67.50	71.30	37.024 8	5.37
14	45	200	600	72.50	66.60	69.55	36.822 5	4.17
15	45	200	700	72.20	63.70	67.95	36.592 8	6.01
16	45	300	500	70.20	64.10	67.15	36.514 0	4.31
17	45	300	600	71.90	66.00	68.95	36.746 8	4.17
18	45	300	700	69.60	59.30	64.45	36.101 2	7.28
19	90	100	500	66.20	66.70	66.45	36.449 7	0.35
20	90	100	600	72.40	75.10	73.75	37.350 9	1.91
21	90	100	700	75.80	64.40	70.10	36.828 1	8.06
22	90	200	500	68.70	64.10	66.40	36.427 7	3.25
23	90	200	600	71.80	61.10	66.45	36.365 4	7.57
24	90	200	700	68.90	59.80	64.35	36.105 8	6.43
25	90	300	500	64.00	56.60	60.30	35.557 3	5.23
26	90	300	600	65.10	63.60	64.35	36.169 2	1.06
27	90	300	700	64.20	59.60	61.90	35.815 8	3.25

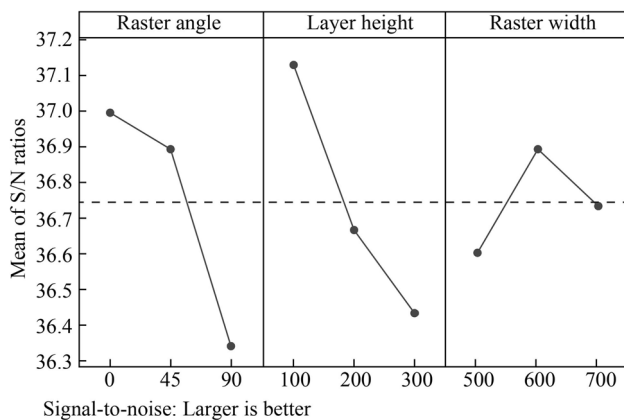


Fig. 3 Main effect plot for flexural strength

biodegradation does not contribute to the aggregate sum of the atmospheric carbon dioxide. Therefore, the effect on nature during the production and disposal of PLA and its carbon impression is reduced compared with other petro-based polymers [23, 24].

PLA exhibit mechanical properties that are comparable with those of petro-based commercial polymers. Further, it can be decomposed in the human body and in the environment. The toxicity of its decomposition products, which are lactic acid and its oligomers, is low. The functionality of hydrolytic degradability and the specific low toxicity of the resultant product are useful for environmental, biomedical, and pharmaceutical applications [25, 26]

PLA is a typical polymer used in FFF-technology-based 3D printers, and is typically available as a 3D printable filament. All the test specimens were printed using a PLA filament (Esun 3d filament, Shenzhen, China). Table 1 shows the properties of the PLA filament as per the manufacturer's technical data sheet.

2.3 Process parameters

The flexural strength of the FFF-printed part is primarily dependent on the selection of the process variables. Hence,

in the present study, three process variables are selected for the investigation on flexural strength: raster angle, layer height, and raster width. Tables 2 and 3 show the selected process variables and their levels along with the fixed process parameters that are considered during the printing of flexural specimens.

2.4 Flexural test

The objective of the study is to understand the flexural behavior of FFF-built PLA parts, and to study the effects of various build parameters including raster angle, layer height, and raster width on the flexural properties.

The specimens are built with PLA material using the Omega Dual extruder machine. The specimen in this study is a rectangular block of dimensions 127 mm × 12.7 mm × 3.2 mm to exhibit flexural strength, as shown in Fig. 1.

The three-point bend test was performed on a Tinius Olsen H50KL universal testing machine according to the ASTM D790 standard (as shown in Fig. 2a). Figure 2b shows the experimental setup for the flexural test.

The flexural tests measure the flexural strength and flexural modulus of the specimens. The rate of loading (R) in the test was 1.36 mm/min at 0.01/min rate of straining, and is calculated using

$$R = \frac{ZL^2}{6d}, \quad (1)$$

where L and d are the length of the span and depth of the test specimen, respectively.

In accordance with the test standard, the span length (L) between the supporting pin was adjusted to 51.2 mm in this testing. The load (P) was applied using a loading pin at the center of the span length. The surface begins to bend gradually and the stress vs. strain data for the test specimen are plotted by the inbuilt Horizon software. The stress (σ) caused by the bending moment in a three-point bend test is flexural stress, and it is calculated using

Table 5 Analysis of variance for flexural strength

Source	DF	SS	MS	F-value	P-value	Contributions/%
Raster angle	2	2.243 6	1.121 78	18.67	0.001	25.76
Layer height	2	2.266 5	1.133 23	18.86	0.001	26.02
Raster width	2	0.389 5	0.194 75	3.24	0.093	4.47
Raster angle × layer height	4	0.817 9	0.204 46	3.40	0.066	9.39
Raster angle × raster width	4	1.752 3	0.438 09	7.29	0.009	20.12
Layer height × raster width	4	0.757 8	0.189 45	3.15	0.078	8.70
Error	8	0.480 8	0.060 10			
Total	26	8.708 3				

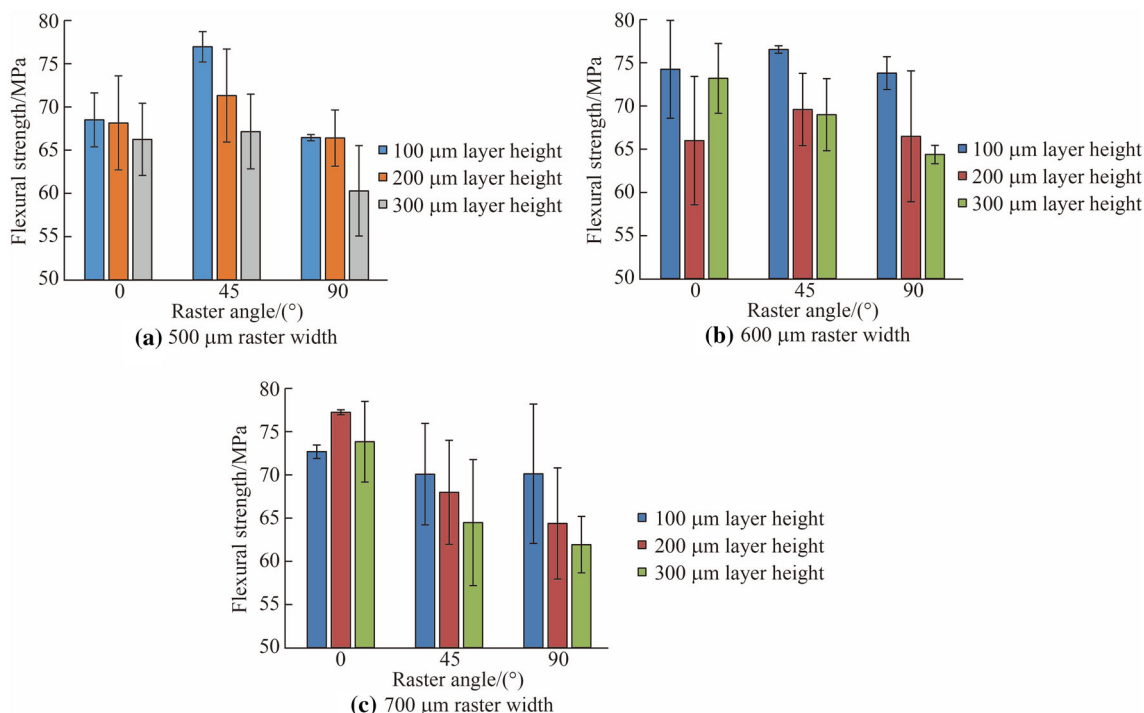


Fig. 4 Effect of raster angle on flexural strength

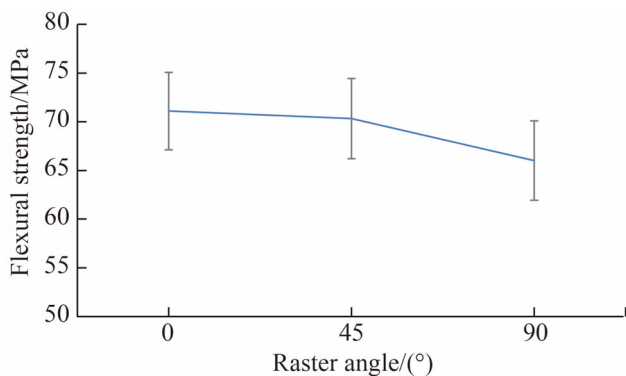


Fig. 5 Mean effect of raster angle on flexural strength

$$\sigma = \frac{3PL}{2bd^2}, \tag{2}$$

where *b* and *d* are the width and depth of the tested specimen, respectively.

The flexural strain (ϵ) is defined as the nominal fraction change in the length of an element on the outer surface of the test specimen at mid-span, where the maximum strain occurs. It can be calculated for any deflection using

$$\epsilon = \frac{6Dd}{L^2}, \tag{3}$$

where *D* is the maximum deflection at the center of the specimen. The upper surface in contact with the loading pin experience compression, whereas the bottom surface in

contact with the supporting pins experiences tension. When the maximum load is reached, a crack is initiated on the bottom surface and propagates towards the upper surface, causing the specimen to break or deform primarily. The test ends when the specimen breaks or once the material reaches 5% strain, whichever occurs first.

3 Results and discussions

All the experiments were performed as per the experimental design shown in Table 4. In the present experimental study, three factors have been varied at three levels. Hence, as per the full factorial experiential design, 27 experiments must be performed with different experimental conditions, as shown in Table 3. All the experiments were performed twice to accommodate the noise effect on the response. The experimental results obtained for both trials along with the S/N ratio and the standard deviation is shown in Table 4.

A higher flexural strength is desirable. Therefore, the primary effect plots have been constructed using the S/N ratio with the-larger-the-better conditions. From Fig. 3, it is apparent that the layer height is the most influencing process variable on the flexural strength, followed by the raster angle and raster width. Figure 3 indicates the graph of the S/N ratio for all trials, in which a steep curve represents the most influencing process variable. The larger S/N ratio

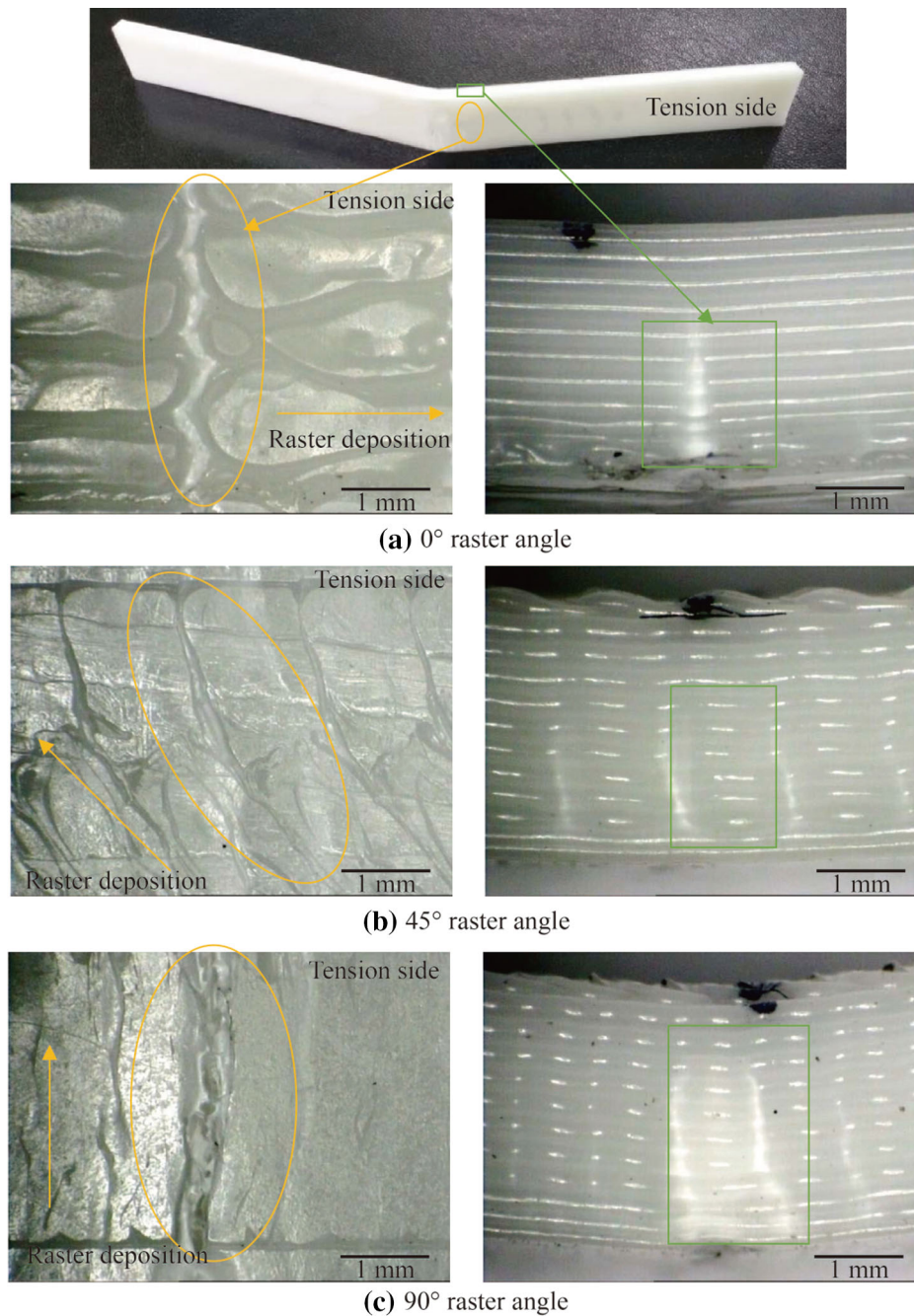


Fig. 6 Microscopic image of the specimen after flexural testing for various raster angle (layer height 300 μm and raster width 500 μm)

values of the process variables correspond to the best characteristic output. Hence, the optimal condition to obtain a higher flexural strength is observed at raster angle 0°, layer height 100 μm , and raster width 600 μm .

Further, the analysis of variance (ANOVA) has been performed to analyze the effect of raster angle, layer height, and raster width on flexural strength. The input process variables were analyzed more specifically, and their influences on the flexural strength were studied. In the ANOVA table, the F -value column is also called the

Fisher's F -test value. The higher F -value represents the maximum effect on the flexural strength, whereas the lower value represents the minimal effect on the flexural strength. The ANOVA table shows that the layer height influences the flexural strength the most, followed by the raster angle. The ANOVA has been determined for a 95% confidence interval that is at a 5% significance level. Table 4 describes the ANOVA of flexural strength, where the layer height followed by the raster angle is highly statically significant, with the contributions of 26.02% and 25.76%, respectively.

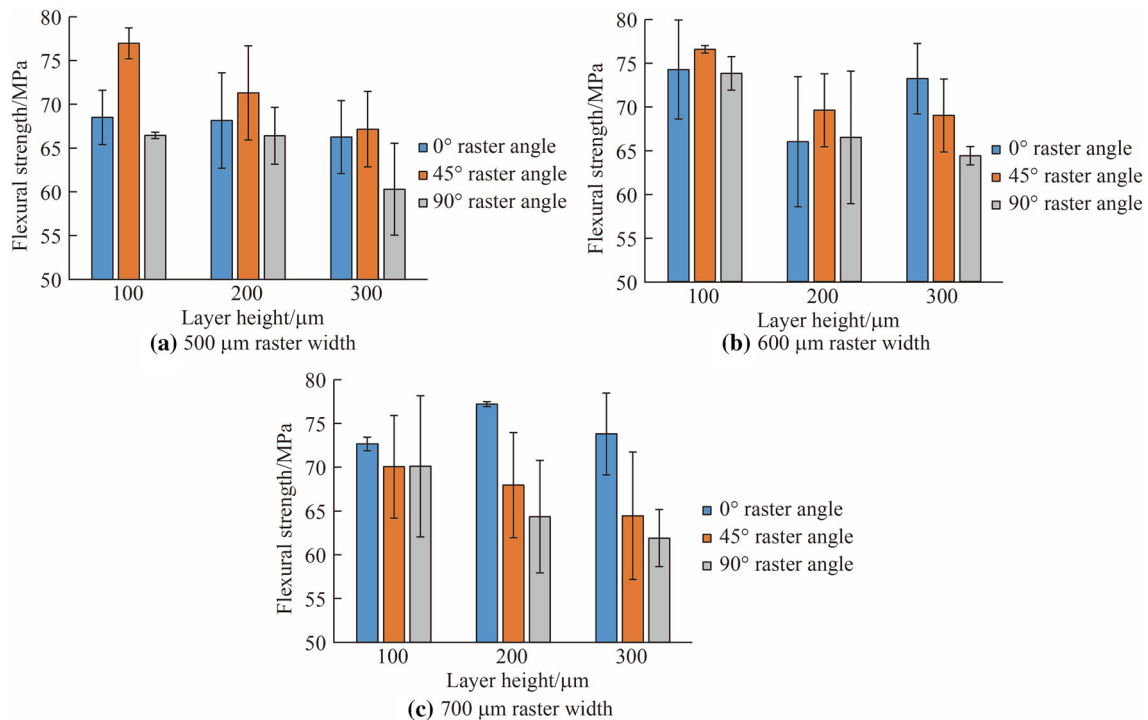


Fig. 7 Effect of layer height on flexural strength

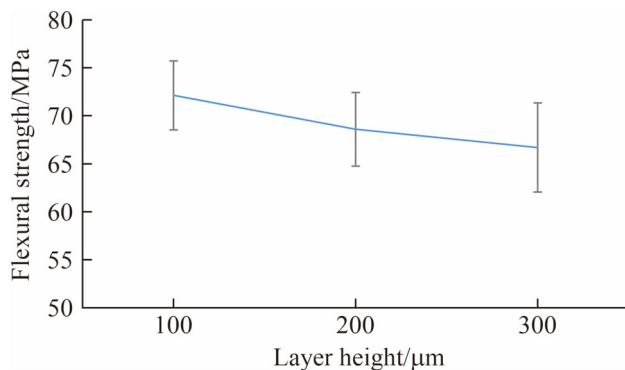


Fig. 8 Mean effect of layer height on flexural strength

The product of raster angle and raster width contributes 20.12% to the output even though it is not significant (see Table 5).

3.1 Effect of raster angle

The effect of the raster angle on the flexural strength of printed PLA is shown in Fig. 4. As shown, in most cases, the flexural strength decreased with the increment in raster angle; however, for the 500-μm raster width, a higher flexural strength was observed with 45° raster angle instead of 0° raster angle.

Figure 5 shows the mean effect of raster angle on the flexural strength of the PLA part. The trend is in

accordance with the flexural strength obtained through the S/N ratio (as shown in Fig. 3). The flexural strength is shown to decrease with increasing raster angle.

From Figs. 3–5, we observed that a higher flexural strength could be obtained at 0° raster angle, and that it decreased with increasing raster angle. The specimen with 0° raster angle offers more resistance to bending because the raster angle exhibits a stronger interlayer bonding compared to other raster angles, and the deposited layers are parallel to the bending plane that offers more resistance to the bending force. The fracture pattern for a specimen with 0° raster angle is shown in Fig. 6a. It reveals that failure is initiated at the tensile side but the pieces are held together by unbroken rasters on the compression side. Crack propagation along the load direction is shown, and it is almost straight for the specimen built with 0° raster angle along the raster deposition direction. Moreover, as the raster angle changes to 45° and 90°, the raster deposited at the respective inclined angle produced a raster of a smaller length under flexural loading, and its resistance to bending decreases. The fracture patterns for specimens with 45° and 90° raster angles are shown in Figs. 6b and 6c, respectively. The specimen with 90° raster angle shows the lesser resistance to bending. Crack propagation along the raster deposition is shown, and it is propagated through the bonding between the rasters that comparatively weakens compared to a monofilament.

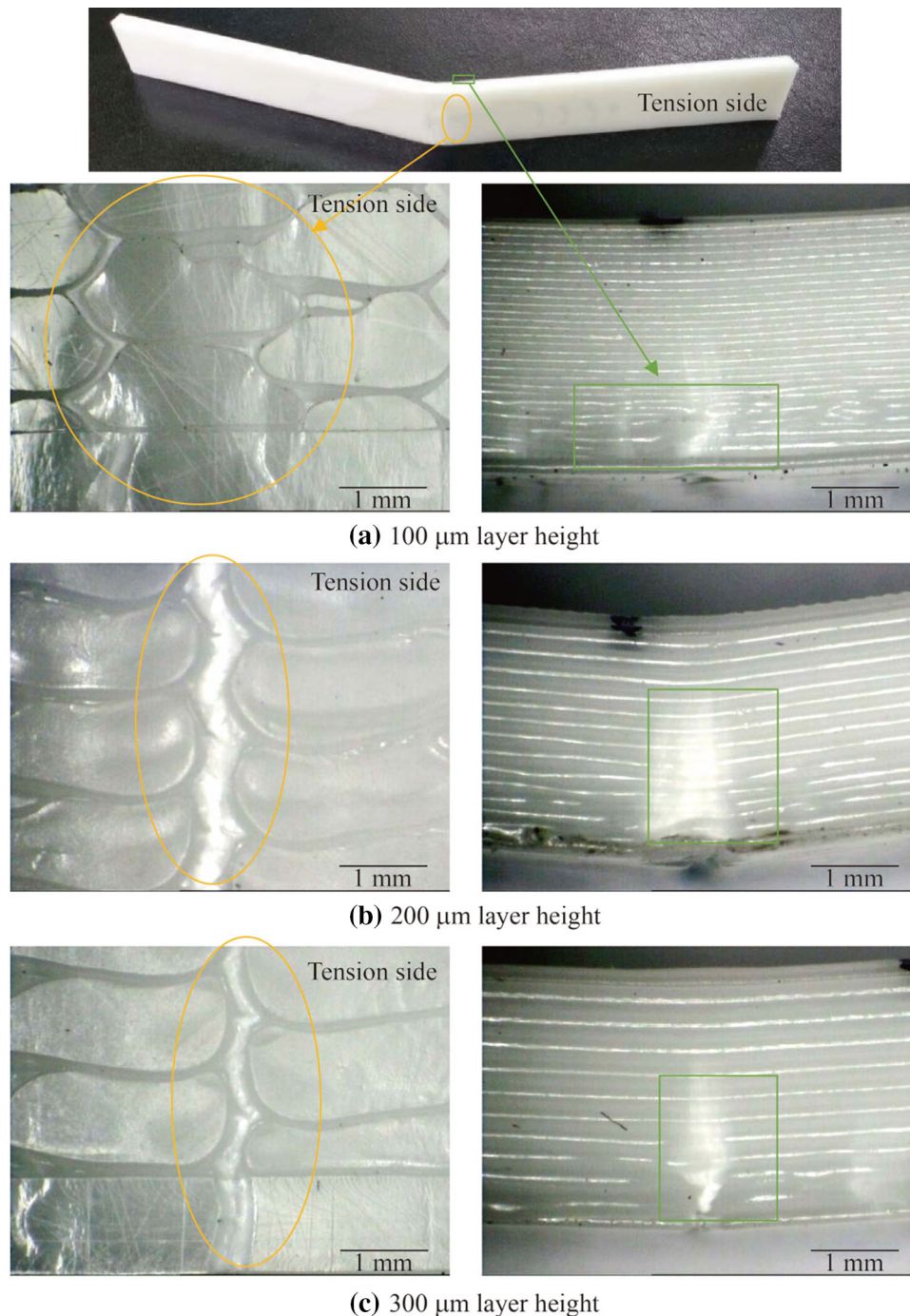


Fig. 9 Microscopic image of the specimen after flexural testing for various layer height (raster angle 0° and raster width $600 \mu\text{m}$)

3.2 Effect of layer height

Figure 7 shows the effect of the layer height on the flexural strength of the printed PLA. As shown, the flexural strength decreased with the increment in layer height.

Figure 8 shows the mean effect of the layer height on the flexural strength of the PLA part. The trend is in accordance with the flexural strength obtained through the

S/N ratio (as shown in Fig. 3). The flexural strength decreased with increasing layer height.

Figures 3, 7 and 8 show that a higher flexural strength can be achieved with $100 \mu\text{m}$ layer height, and a lower flexural strength is observed with $300 \mu\text{m}$ layer height. The flexural strength of the $200 \mu\text{m}$ layer is between these two. A higher flexural strength is found at a lower layer height because of the higher bonding strength between layers. At a

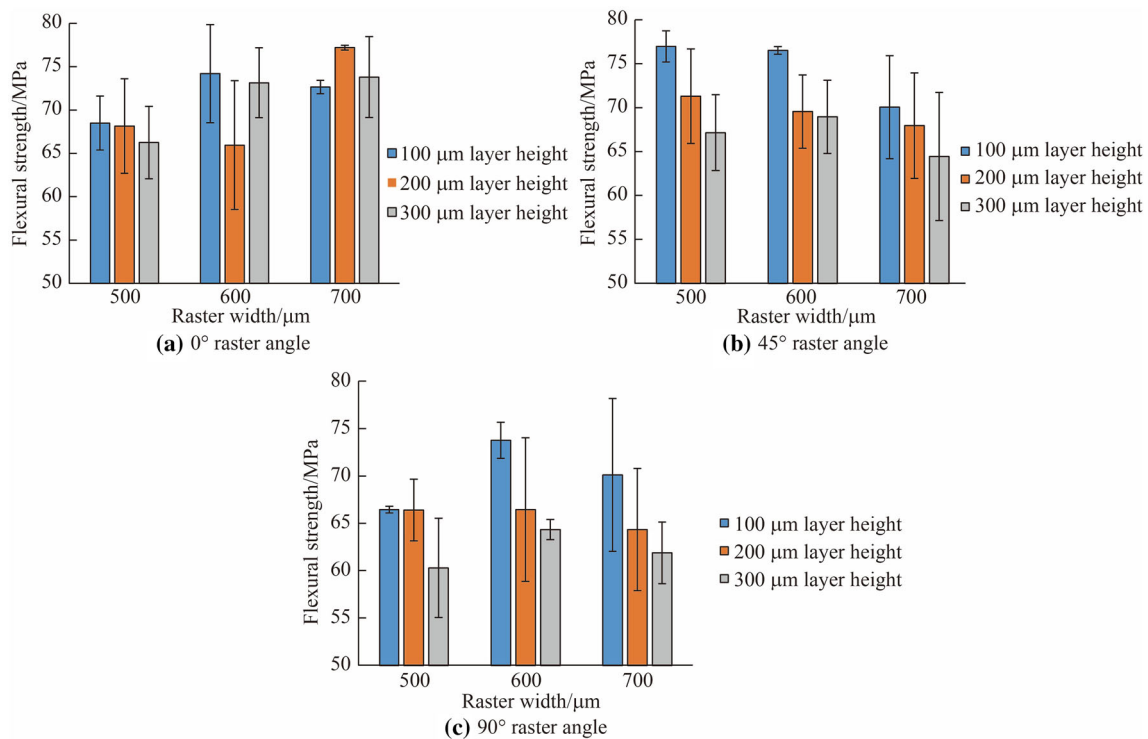


Fig. 10 Effect of raster width on flexural strength

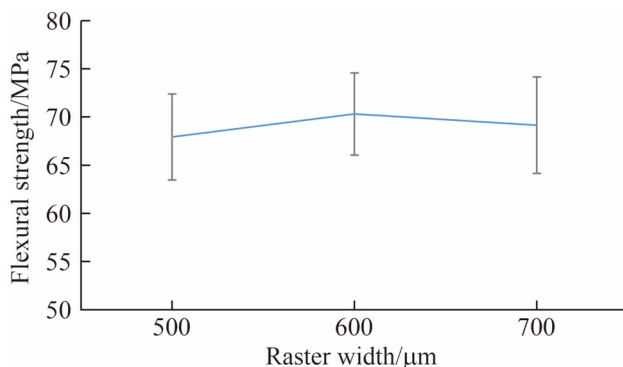


Fig. 11 Mean effect of raster width on flexural strength

lower layer height, larger bonding occurs between the layers, thus resulting in a much stronger bond. At a lower layer height, a molten raster requires a higher extrusion pressure for a proper deposition. The higher pressure generated owing to the lower layer height ensures the contact between the two layers, eventually resulting in a greater bond strength. The fracture pattern for a specimen with 100 μm layer height is shown in Fig. 9a. It shows that failure is initiated at the tensile side but the pieces are held together by unbroken rasters of the compression side. A wide stress whitening is shown, which offers more resistance to the bending load. For the 200 μm and 300 μm layer heights, a small stretching of raster led to a

catastrophically brittle failure, indicating less resistance to bending.

3.3 Effect of raster width

Figure 10 shows the effect of raster width on the flexural strength of the printed PLA. As shown, the flexural strength is increased initially to the optimal point, and subsequently reduced with further increment in the raster width.

Figure 11 shows the mean effect of the raster width on the flexural strength of the PLA part. The trend is in accordance with the flexural strength obtained through the S/N ratio (see Fig. 3). The flexural strength increased with the raster width up to 600 μm; subsequently, it starts decreasing.

Moreover, as shown in Figs. 3, 10, and 11, the flexural strength has been increasing with the raster width up to 600 μm, and it subsequently starts decreasing. At a larger raster width, the raster possesses more thermal mass, owing to which it cools slowly and remains above the glass transition temperature for a longer duration. This improves the bonding between the adjacent raster, thus resulting in a higher bond strength. The raster with a larger width has more contact area between the layers, which improves the bond strength. Catastrophic and brittle failure can be observed for a specimen with 500 μm raster width, as shown in Fig. 12a. The failure initiated from the bottom layers that undergo tensile stretching, but the unbroken

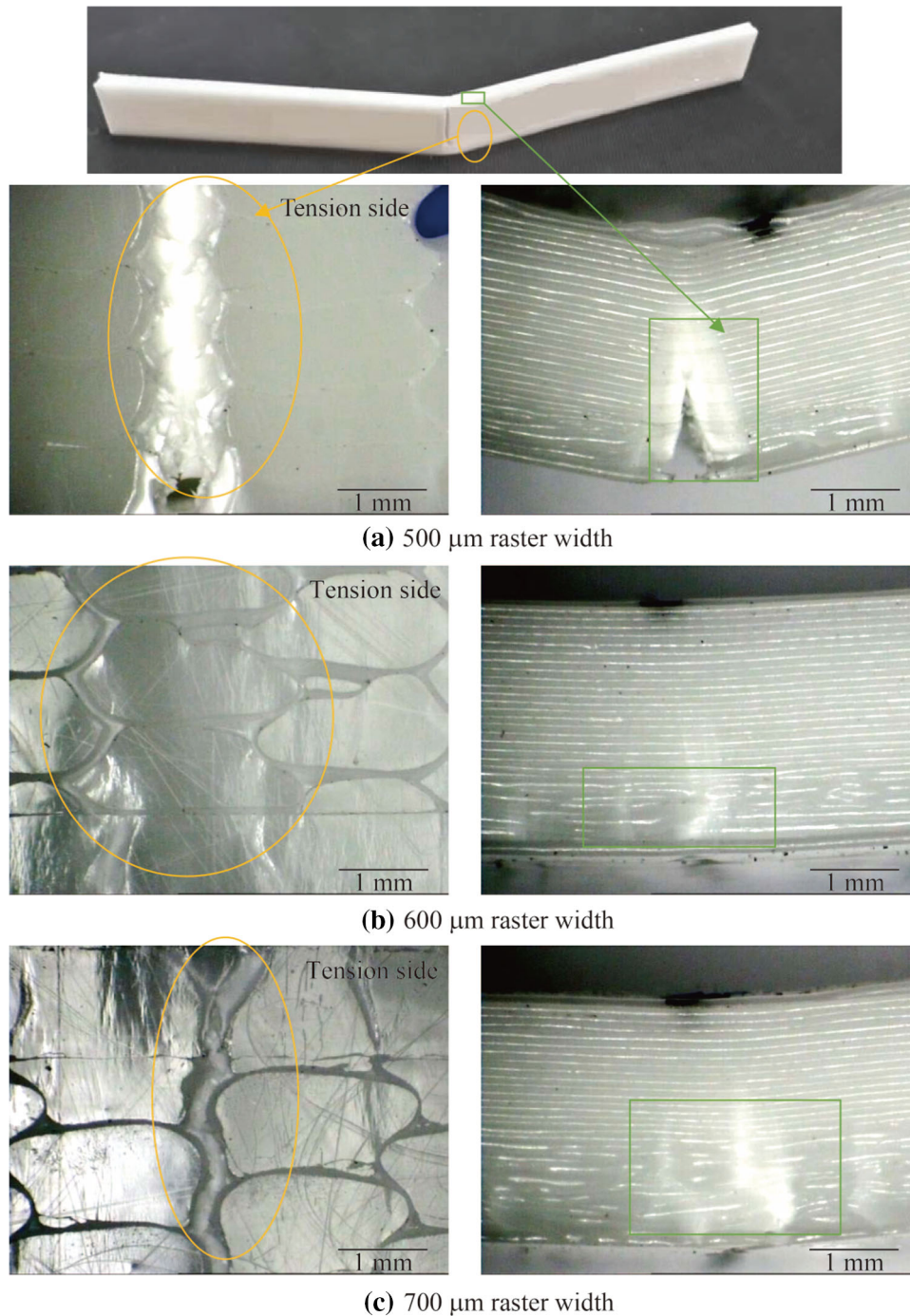


Fig. 12 Microscopic images of the specimen after flexural testing at various raster width (raster angle 0° and layer height 100)

layers on the compression side held the pieces together. Wide stress whitening (see Fig. 12b) is shown for the 600- μm raster width that offers more resistance to bending. A small catastrophic crack opening, as shown for the 700- μm raster width (see Fig. 12c), reduces the flexural strength of the specimen.

4 Conclusions

Investigation of the mechanical properties of FFF-produced parts is emerging, as it has many implications in the field of additive manufacturing. However, the limited mechanical properties of the parts restricted their wide application in many fields. The present work focused on the investigation of the flexural strength of FFF-produced PLA parts under

different printing conditions. The conclusions of the present work are as follows:

- (i) A higher flexural strength was observed at 0° raster angle, 100 μm layer height, and 600 μm raster width.
- (ii) Flexural strength decreased with increasing raster angle. At a 0° raster angle, the failure was primarily due to the stretching and rupture of the deposited beads; meanwhile, for the 45° and 90° raster angles, failure occurred parallel to the raster deposition through the shear bonding between the deposited beads.
- (iii) Flexural strength decreased with increasing layer height. At the lower layer height, more layers were deposited and a higher extrusion pressure was required to deposit a thin layer to improve the bonding between layers, thus ultimately enhancing the flexural strength. Wide stretch marking was observed using a lower layer thickness, indicating the higher resistance to flexural loading.
- (iv) At the intermediate value of the raster width, a higher flexural strength was obtained owing to the higher thermal mass that cools slowly, thus improving the bonding between the rasters and improved the flexural strength.
- (v) The present study can be further extended by studying the effects of process variables such as deposition speed, number of perimeters, bed temperature, and extrusion temperature on the flexural strength of PLA parts.

Reference

1. Francis V, Jain PK (2018) Investigation on the effect of surface modification of 3D printed parts by nanoclay and dimethyl ketone. *Mater Manuf Process* 33:1080–1092
2. Chockalingam K, Jawahar N, Praveen J (2016) Enhancement of anisotropic strength of fused deposited ABS parts by genetic algorithm. *Mater Manuf Process* 31:2001–2010
3. Gill SS, Kaplas M (2009) Comparative study of 3D printing technologies for rapid casting of aluminium alloy. *Mater Manuf Process* 24:1405–1411
4. Liao G, Li Z, Cheng Y et al (2018) Properties of oriented carbon fiber/polyamide 12 composite parts fabricated by fused deposition modeling. *Mater Des* 139:283–292
5. Zou R, Xia Y, Liu S et al (2016) Isotropic and anisotropic elasticity and yielding of 3D printed material. *Compos B Eng* 99:506–513
6. Garg A, Bhattacharya A, Batish A (2016) On surface finish and dimensional accuracy of FDM parts after cold vapor treatment. *Mater Manuf Process* 31:522–529
7. Wu W, Jiang J, Jiang H et al (2018) Improving bending and dynamic mechanics performance of 3D printing through ultrasonic strengthening. *Mater Lett* 220:317–320
8. Mishra SB, Malik R, Mahapatra SS (2017) Effect of external perimeter on flexural strength of FDM build parts. *Arab J Sci Eng* 42:4587–4595
9. Luzanin O, Guduric V, Ristic I et al (2017) Investigating impact of five build parameters on the maximum flexural force in FDM specimens—a definitive screening design approach. *Rapid Prototyp J* 23:1088–1098
10. Mohamed OA, Masood SH, Bhowmik JL (2017) Investigation on the flexural creep stiffness behavior of PC–ABS material processed by fused deposition modeling using response surface definitive screening design. *J Miner Met Mater Soc* 69:498–505
11. Garg A, Bhattacharya A, Batish A (2017) Failure investigation of fused deposition modelling parts fabricated at different raster angles under tensile and flexural loading. *Proc Inst Mech Eng Part B J Eng Manuf* 231:2031–2039
12. Motaparti KP, Taylor G, Leu MC et al (2017) Experimental investigation of effects of build parameters on flexural properties in fused deposition modelling parts. *Virtual Phys Prototyp* 12:207–220
13. Rahman KM, Letcher T, Reese R (2015) Mechanical properties of additively manufactured PEEK components using fused filament fabrication. In: *Proceeding of the ASME International Mechanical Engineering Congress and Exposition (IMECE2015)*. Houston, Texas, November 13–19
14. Christiyan KJ, Chandrasekhar U, Venkateswarlu K (2016) Flexural properties of PLA components under various test condition manufactured by printer. *J Inst Eng (India) Ser C* 114:1–5
15. Knoop F, Kloke A, Schoeppner V (2017) Quality improvement of FDM parts by parameter optimization. *AIP Conf Proc* 1914:190001
16. Sood AK, Ohdar RK, Mahapatra SS (2010) Parametrical appraisal of mechanical property of fused deposition modelling processed parts. *Mater Des* 31:287–295
17. Guan HW, Savalani MM, Gibson I et al (2015) Influence of fill gap on flexural strength of parts fabricated by curved layer fused deposition modeling. *Proc Technol* 20:243–248
18. Dawoud M, Taha I, Ebeid SJ (2016) Mechanical behaviour of ABS: an experimental study using FDM and injection moulding techniques. *J Manuf Process* 21:39–45
19. Durgun I, Ertan R (2014) Experimental investigation of FDM process for improvement of mechanical properties and production cost. *Rapid Prototyp J* 20:228–235
20. Liu X, Zhang M, Li S et al (2017) Mechanical property parametric appraisal of fused deposition modeling parts based on the gray taguchi method. *Int J Adv Manuf Technol* 89:2387–2397
21. Huang B, Meng S, He H et al (2018) Study of processing parameters in fused deposition modeling based on mechanical properties of acrylonitrile-butadiene-styrene filament. *Polym Eng Sci*. <https://doi.org/10.1002/pen.24875>
22. Es-Said OS, Foyos J, Noorani R et al (2000) Effect of layer orientation on mechanical properties of rapid prototyped samples. *Mater Manuf Process* 15:107–122
23. Pivsa-Art W, Chaiyasat A, Pivsa-Art S et al (2013) Preparation of polymer blends between poly (lactic acid) and poly (butylene adipate-co-terephthalate) and biodegradable polymers as compatibilizers. *Energy Proc* 34:549–554
24. Zhang J, Wang S, Qiao Y et al (2016) Effect of morphology designing on the structure and properties of PLA/PEG/ABS blends. *Colloid Polym Sci* 294:1779–1787
25. Choe II, Lee JH, Yu JH et al (2014) Mechanical properties of acrylonitrile-butadiene-styrene copolymer/poly (l-lactic acid) blends and their composites. *J Appl Polym Sci* 131:40329.1
26. Jo MY, Ryu YJ, Ko JH et al (2012) Effects of compatibilizers on the mechanical properties of ABS/PLA composites. *J Appl Polym Sci* 125:E231–E238